ARTICLE

Optimization of a Solar Chimney with a Horizontal Absorber for Building Ventilation: A Case Study

El Hadji I Cisse[1,*], Baye Alioune Ndiogou[1,2], Soumaïla Tigampo[1], Ababacar Thiam[1,3] and Dorothé Azilinon[1]

[1](L3EPI) Laboratory of ESP-UCAD, Dakar, Senegal

[2]Center for Energy Research and Sustainability, DAUST, Dakar, Senegal

[3]Universiy Alioune Diop of Bambey, Bambey, Senegal

[*]Corresponding Author: El Hadji I Cisse. Email: elhadjiibrahima.cisse@ucad.edu.sn

ABSTRACT

A study is conducted to optimize the geometry of a solar chimney equipped with a horizontal absorber in order to improve its performances in relation to the provision of ventilation. The problem is tackled through numerical solution of the governing equations for mass, momentum and energy in their complete three-dimensional and unsteady formulation. The numerical framework also includes a turbulence model (k-ε) and a radiant heat transfer (DO) model. Moreover, a Multi-Objective Genetic Algorithm (MOGA) is employed to derive the optimal configuration of the considered solar chimney. It is shown that an air velocity of 0.2 m/s can be obtained. This value is the minimum allowed air velocity according to the ASHRAE's (American Society of Heating, Refrigerating and Air-Conditioning Engineers) adaptive comfort approach.

Nomenclature

Greek letters	Units
absorptivity	
dissipation rate	
Reynolds stress tensor	
turbulence kinetic energy	
Density	(Kg/m^3)
Stepan's coefficient	$(W/m^2/K^4)$
turbulent Prandtl numbers for	k
turbulent Prandtl numbers for	ε
Thermal Expansion Coefficient	$(1/K)$

1 Introduction

Fossil energy consumption is increasing to the point where the resource is nowadays tending to be exhausted underground. This situation has raised awareness of the need to use alternative sources.

Solar energy is a source of energy abundantly available in sub-Saharan Africa. In the case of Senegal, the solar potential is 3000 h per year and the overall average energy of 5.8 kWh/m^2.

The building is the most energy-intensive component in Africa. This energy intensity is due to the heavy use of ventilation and air conditioning systems for thermal comfort. Whether horizontal or sloped, these roofs absorb a large amount of energy. Several alternatives are possible and have been proposed for years (insulation, green roof, ventilated roof with high point outlet, roof with high inertia bricks with natural ventilation systems to evacuate heat). According to the adaptive approach, comfort depends on room temperature, average radiant temperature, and air velocity [1].

However, the economic and social situation pushes people to build concrete. This material is known for its high conductivity and is not adapted to our climate. The material increases the average radiant temperature of the interior walls—especially the roof, which is the side receiving the most heat from the sun.

Therefore, to influence comfort, the only alternative for already built houses is to increase the air velocity in the building and lower the temperature of the walls. Nevertheless, according to the adaptive approach, mechanical ventilation is prohibited.

However, solar chimneys with horizontal absorbers are more suitable for inducing natural ventilation while shading the roof. This SC is why we have optimized the adaptation of a solar chimney with a horizontal absorber for the natural ventilation of buildings in the sub-Saharan zone, particularly Senegal.

Solar chimneys have been used for ventilation in buildings for three decades. They fall into the "solar chimney power plant" and the solar roof chimney. The first is for power generation, and the second category is for passive ventilation.

Many studies have been conducted in this area, both experimentally and theoretically, whereas experimental studies are mainly focused on small-scale systems [2].

Italian famous artist and genius Leonardo da Vinci (1452–1519) first used the concept of utilizing the air rising upward to create rotation. He used the hot air rising in a chimney to drive a windmill that rotates his roasting spit connected to the windmill.

The power output profile correlates closely with the solar insolation profile during daytime for this prototype plant without an additional storage system, while there is still an updraft during nighttime due to the thermal storage capacity of natural soil, which can be used to produce power during some hours of the night (Haaf, 1984). Krisst (1983) built a courtyard solar chimney (S.C.) power setup with 10 W power output. The collector base diameter and S.C. height were 6 and 10 m, respectively. In 1985, a micro-scale model with an S.C 2 m high and 7 cm in diameter and a 9 m^2 collector was built by Kulunkin Turkey (Kulunk, 1985) [3].

Kinan et al. [4] experimented with the Small Scale Solar Updraft Power Plant. With two types of collector geometry (edge and circular), they reached an output velocity of 1.3 m/s.

In their works, Balijepalli et al. [5] have developed a small scale solar chimney power plant (SCPP). The maximum air velocity below and above the turbine was 4.7 and 5.5 m/s, and the average was 2.18 and 2.98 m/s, respectively. The maximum pressure drop of 4 N/m^2 was noticed across the wind turbine. The theoretical and actual power outputs were 1.37 and 0.82 W, respectively. Chimney and overall plant efficiencies were estimated at 0.0187% and 0.0128%, respectively.

Nsaif [6] studied a numerical simulation of an SCPP through three-dimensional axisymmetric modelling. The study introduces an insight into the performance enhancement methods and finds the best configuration of an SCPP model, which will be the basis of a detailed prototyping process. Based on the numerical results, the best configuration of the SCPP has been found as the diverging chimney, which enhances the generated power. The maximum impact on the performance is found to be by the chimney tower radius, and the collector height

and inclination are found to have optimum values considering performance. According to the obtained results, the best performance for the SCPP was obtained with 3.5 m chimney height, 30 cm tower diameter, 400 cm of collector diameter with 6 cm height and zero inclination angle.

Azizi et al. [7] have aimed to investigate the performances of solar chimneys. A small-scale solar chimney power plant prototype was built in Ouargla University, Algeria. This study evaluates the performances of a solar chimney and the effects of the chimney height on the chimney efficiency and power output. The study found that the air velocities measured at the chimney inlet agree with the CFD model's predicted ones. The simulation results show a recirculation zone at the collector's inlet with negative velocities, which causes a reduction in the solar chimney performance. A maximum air velocity of 1.6 m/s in the entry of the chimney was observed. These results show that solar chimney technology is very suitable for hot and arid zones like southeast Algeria.

Nguyen et al. [8] have studied a solar chimney with a horizontal absorber surface in their paper. A CFD (Computational Fluid Dynamic) model predicted its performance in the induced air flow rate through the channel and the thermal efficiency. The factors include the heat flux and significant dimensions of the chimney: the absorber surface's length, the air channel's gap, and the height and width of the inlet and outlet sections. The results show that increasing all examined factors enhances the flow rate but slightly affects thermal efficiency.

For their part, Layeni et al. [9] used a solar chimney with a horizontal absorber to produce both electricity and ventilation in a building. The results showed that the mass flow of the room increased by 30.1 kg/s with a sensor induced wind of 1 to 8 m/s.

This article will study the feasibility of integrating a solar chimney with horizontal absorber for the natural ventilation of buildings in the Saharan zone.

2 Model of the Ventilation System

The concept combines a solar chimney power plant and a greenhouse. This technology uses the energy from the sun collected by the horizontal ceiling of the building to ventilate the building. The analysis begins by taking the ceiling as a heat collector, then analyses downward conduction heat transfer and natural convection (Fig. 1).
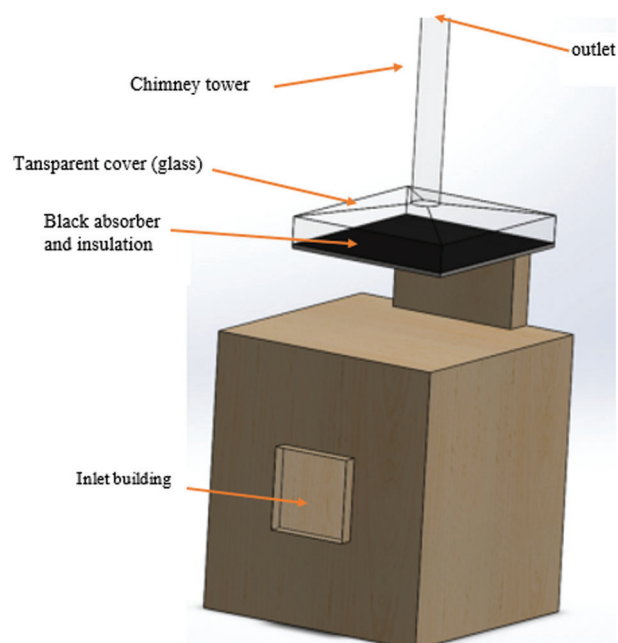

Figure 1: Drawing of the building topped by a solar chimney with horizontal absorber

2.1 Physical Configuration

The physical configuration of this study, shown in Fig. 1, is located in Dakar (a city in the far West of Senegal and Africa), with a longitude and latitude of 17°26′38″ West, 14°41′37″ North, respectively. The average summer temperatures are between 33°C maximum and 24°C minimum, the average wind velocity is 3–8 m/s, and the average global radiation varies from 800 to 900 W/m².

The solar's height conditions the choice to absorb horizontally during the day is high. Therefore, horizontal surfaces receive a large amount of solar radiation flux (Fig. 2).
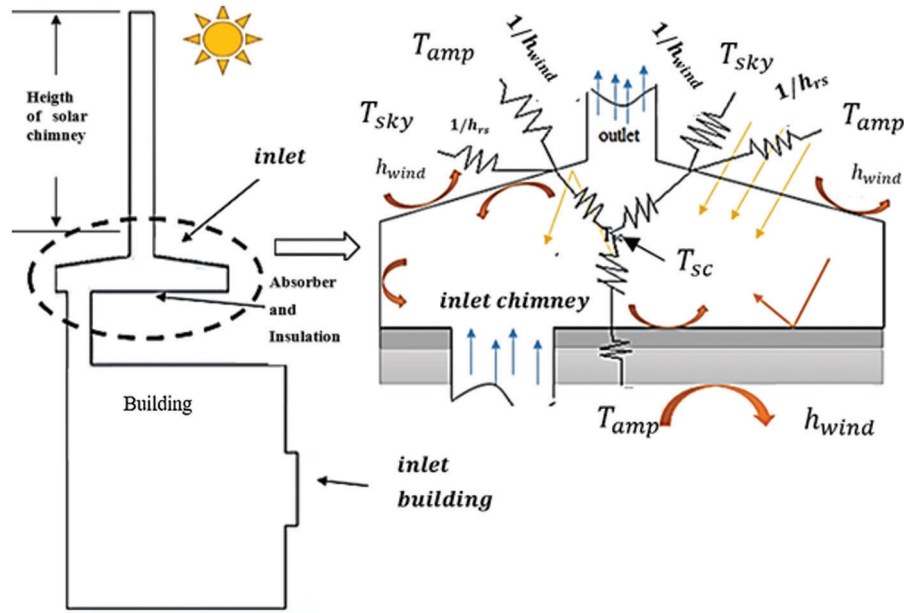

Figure 2: Physical model of solar chimney with horizontal absorber

The mathematical model was established based on the principles of the energy balance on the different parts of the solar chimney. Due to the complex phenomena that occur in the thermal when heat is added to a fluid, fluid density varies with temperature. This variation of fluid density creates an Archimedes thrust called natural convection (or free convection). In natural convection, the force of the flow induced by the Archimedes thrust is measured by the Rayleigh value as follows:

$$Ra = \frac{g\beta\Delta T L^3 \rho}{\mu\alpha} \tag{1}$$

The configuration of our hybrid system is as it straddles a sloping solar chimney on a roof and a solar chimney power plant.

3 Numerical Modelling

The continuity equation is written as follows:

$$\frac{\partial(\rho)}{\partial t} + \nabla(\rho\vec{V}) = 0 \tag{2}$$

The momentum equation is written as follows:

$$\frac{\partial(\rho\vec{V})}{\partial t} + \nabla(\rho\vec{V}.\vec{V}) = \nabla.\left(\overline{\overline{\tau}}\right) - \nabla.(p) + \rho\beta\left(T - T_{ref}\right)\vec{g} \tag{3}$$

In this equation, the Boussinesq buoyancy model is activated. Where ρ is the static pressure, I is the unit tensor, and T_{ref} is the reference temperature.

The term τ presents the shear tensor, which is calculated from the following equation:

$$\overline{\overline{\tau}} = \mu\left(\nabla.\vec{V}\right) + \left(\nabla.\vec{V}\right)^t - \frac{2}{3}\left(\nabla.\vec{V}\right)I \tag{4}$$

The energy equation is written as follows:

$$\frac{\partial(\rho E)}{\partial t} + \nabla\left(\rho(E+p).\vec{V}\right) = \nabla\left(\lambda_{eff}\nabla T - \sum h_j \vec{J}_j + \tau\vec{V}\right) + S \tag{5}$$

where E is the total energy, λ_{eff} the effective heat conduction coefficient, h_j the enthalpy, J_j the diffusion flux of species, and S the term of heat source.

The second last term of Eq. (5) is turbulent stress, evaluated by two equations $k - \varepsilon$.

The solar chimney consists of an opaque and semi-transparent surface. The wavelengths at which these emit must be taken into account.

For this purpose, the Non-grey model was used with both strips. One corresponds to solar radiation $(0 < (\lambda)lamda < 2.7\ \mu m)$ and the other to thermal radiation $(2.7 < (\lambda)lamda < 1000\ \mu m)$.

3.1 Boundary Conditions and Solution Method

The main boundary conditions for studied S.C. are indicated in Fig. 3. The environment's temperature is set as 305 K. For the roof of the collector, both heat transfer via convection and long-wave radiation is considered by using combined convection and external radiation boundary conditions.
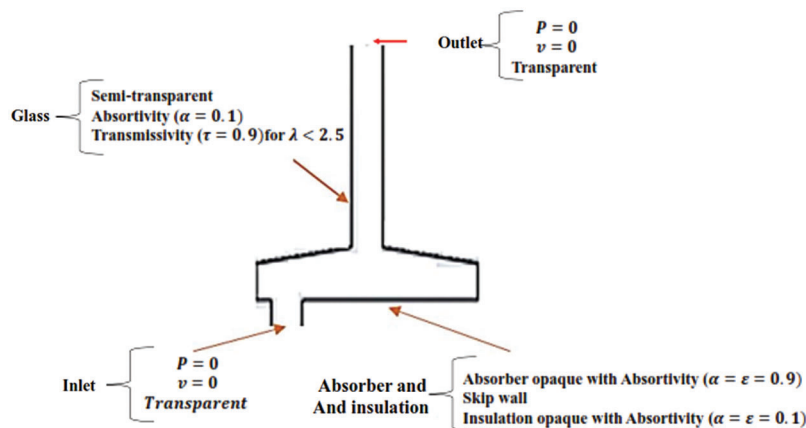

Figure 3: Boundary conditions

Meanwhile, the inner surfaces of the collector and upper surfaces of the ground have a fluid or solid region on each side and are called "two-sided walls". The collector inlet and chimney outlet are assigned as pressure inlet and pressure outlet, respectively, with their values set as 0 Pa to simulate the buoyancy-driven flow in S.C.

The SIMPLE algorithm is selected as the pressure–velocity coupling scheme. The Body Force Weighted algorithm is chosen as the discretization method for the pressure term. The structured grid is adopted, and grid independence has been investigated by analyzing cases with different mesh sizes until consistent results are achieved. The grid is refined in the transition section connecting the collector and chimney because large gradients appear in this region.

The materials used in numerical simulations are listed in Table 1.

The numerical results were verified by a grid independence study, which was carried out on four grid densities with hexahedral cells ranging from 51,624 to 2,127,612 elements, as shown in Fig. 4. The experimental device used to validate our numerical model is installed on the university campus of the National Institute of Technology Warangal (NITW), India. Fig. 5 shows the dimensions of this small scale solar chimney power plant.

Table 1: Thermophysical properties of materials

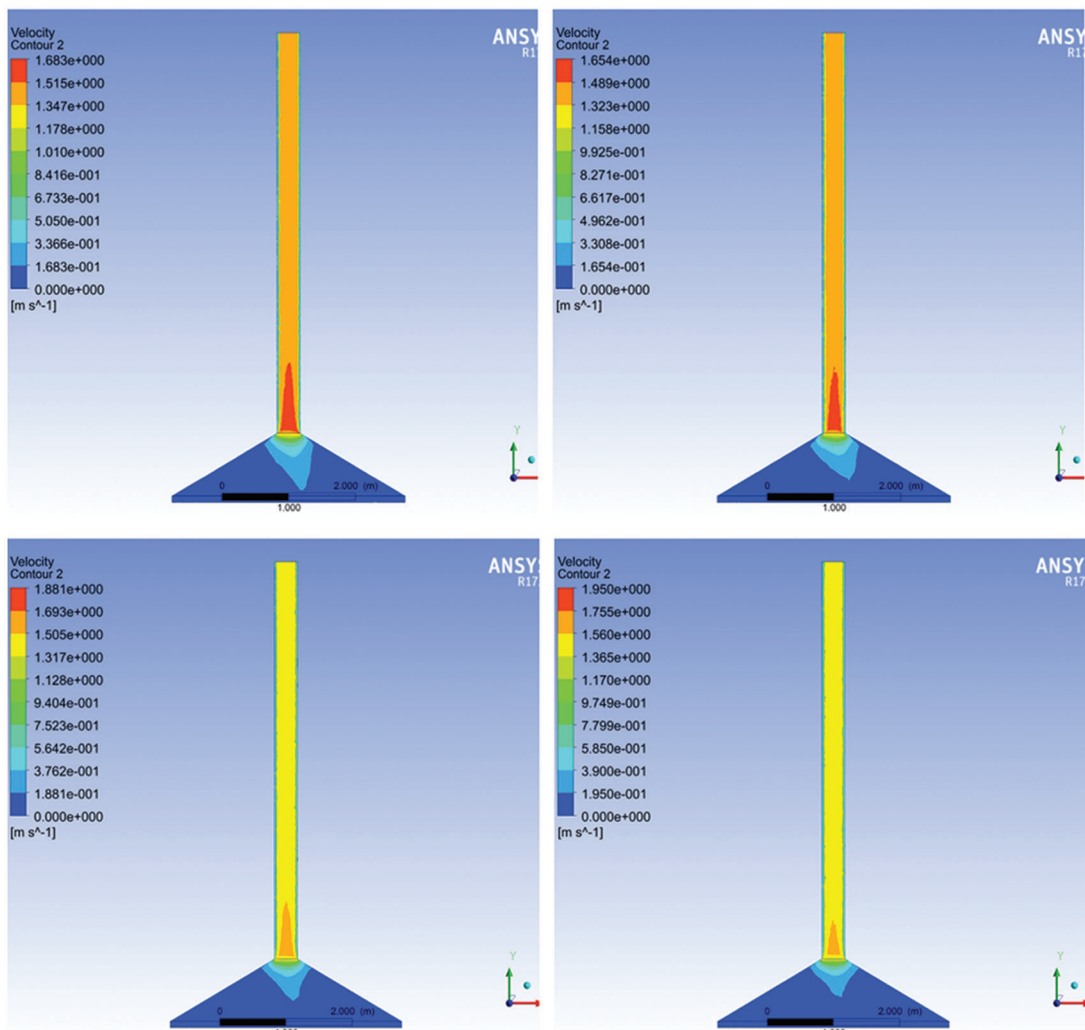| Properties	Air	Glass	Steel	Wood	Insulation
Density (kg/m^3)	Boussinesq = 1,18	2220	8030	700	10
Cp ((specific heat) (J/kg.K))	1006,4	830	502,48	2310	830
Thermal conductivity (W/(m.s))	0,0424	1,15	16,27	0,173	0,1
Viscosity (kg/(m.s))	1,7894E–5	–	–	–	–
Thermal Expansion Coefficient (1/K)	0,00335	–	–	–	–

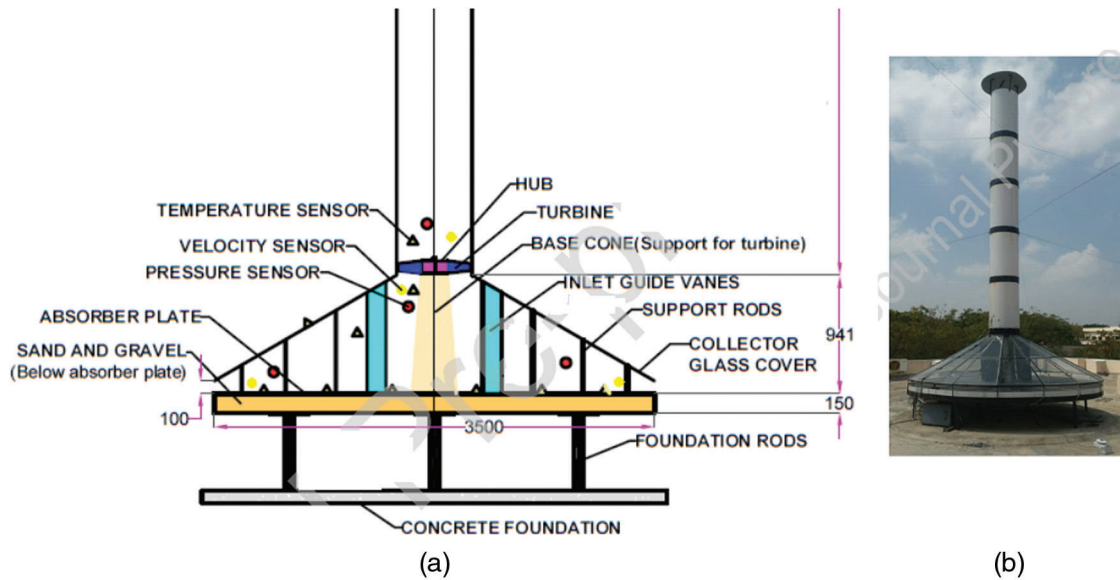**Figure 4:** Velocity maps for grid mesh resolution

Figure 5: (a) View of solar chimney power plant (All dimensions are in mm) (b) A SCPP setup (All dimensions are in mm) (b) A SCPP setup developed at CAM Building, NIT Warangal, Telangana State, India [5]

3.2 Mesh Effect and Grid Resolution on Velocity

The mesh generation (Fig. 6) is a decisive step in the simulation. In this paper, the absorber and the glass are the more critical part of the system (Table 2). The near-wall regions have meshed with a progressive transition.
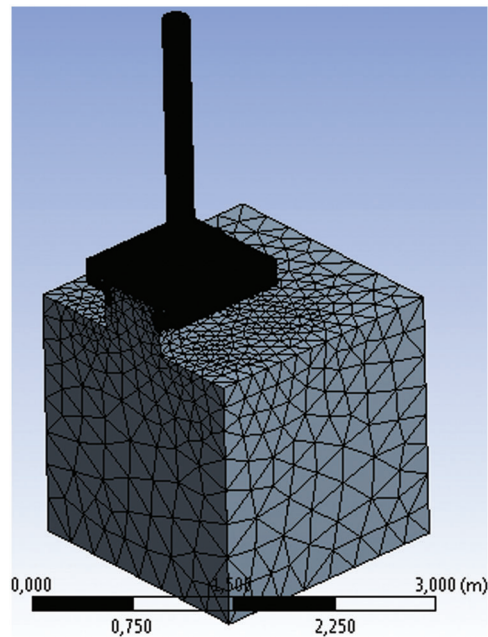

Figure 6: Mesh of the geometry

Table 2: Grid resolution and basics assumptions for the CFD simulations

Elements	Velocity	Turbulence	Solutions methods
3235	0,399685	k	Simple
3181	0,411096	RNG	PRESTO
174128	0,398915	Standard wall functions	Momentum (second-order)
		Full buoyancy effects	Turbulent Kinetic Energy (second order)
			Turbulent Dissipation (second order upwind)
			Energy (second order)

4 Results and Discussions

In order to understand the internal velocity after using the solar chimney with horizontal absorber, The simulation is done when the sun is in its zenith. The Direct Normal Irradiation (DNI) value is 810 W/m^2.

The velocity distribution in the building is shown in the following Fig. 7. The steady-state simulation shows that the adaptive comfort velocity is achieved in the working area.
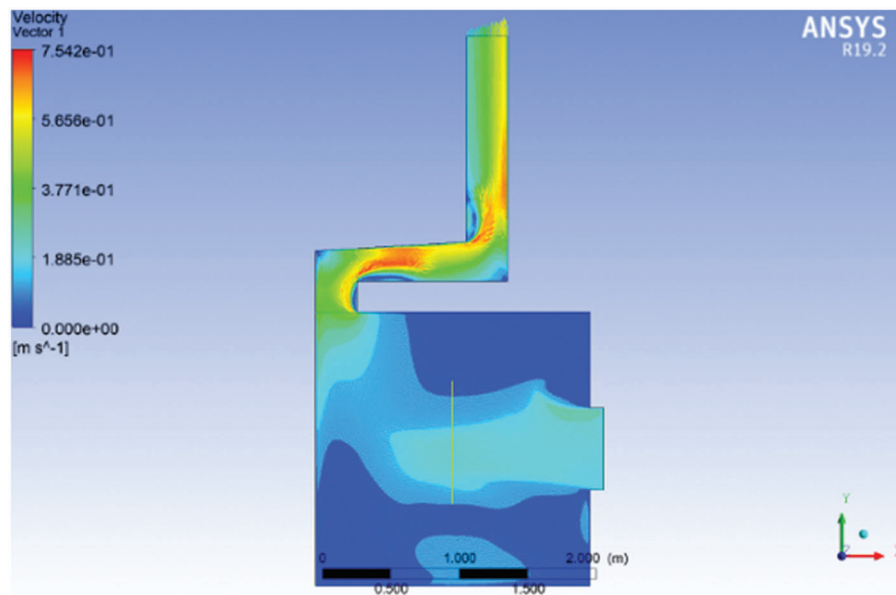

Figure 7: Velocity maps in the building

A study of the local geometric parameters allows us to know their influences on the performance of the solar chimney. Fig. 8 shows the influence of these parameters on the air velocity in the living area. The two most influential parameters are the outlet diameter and the chimney's height. Fig. 9 shows the response of the various geometric parameters concerning the velocity in the living zone. The algorithm (MOGA) favours the two parameters: the height and diameter of the chimney.
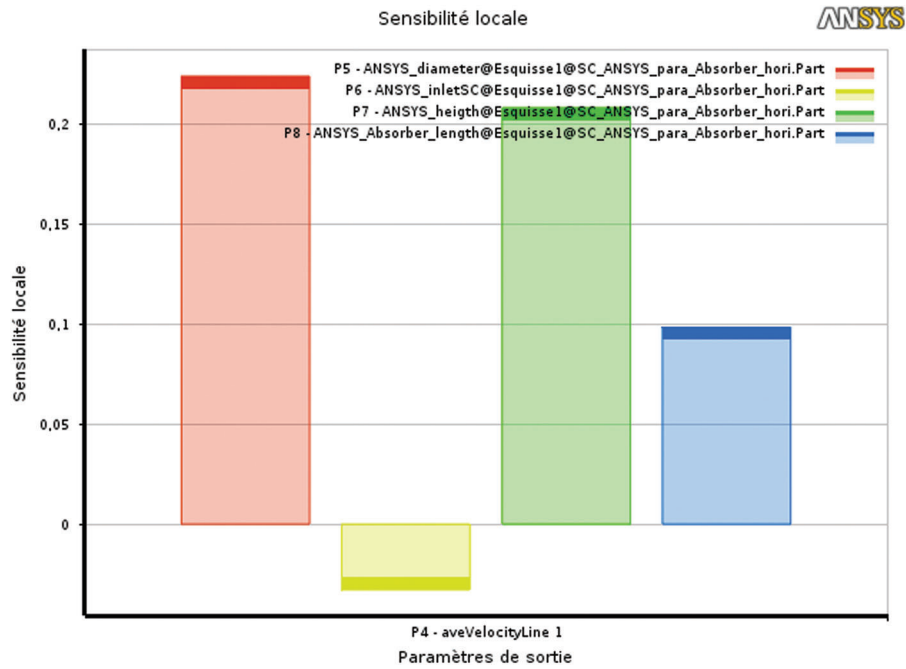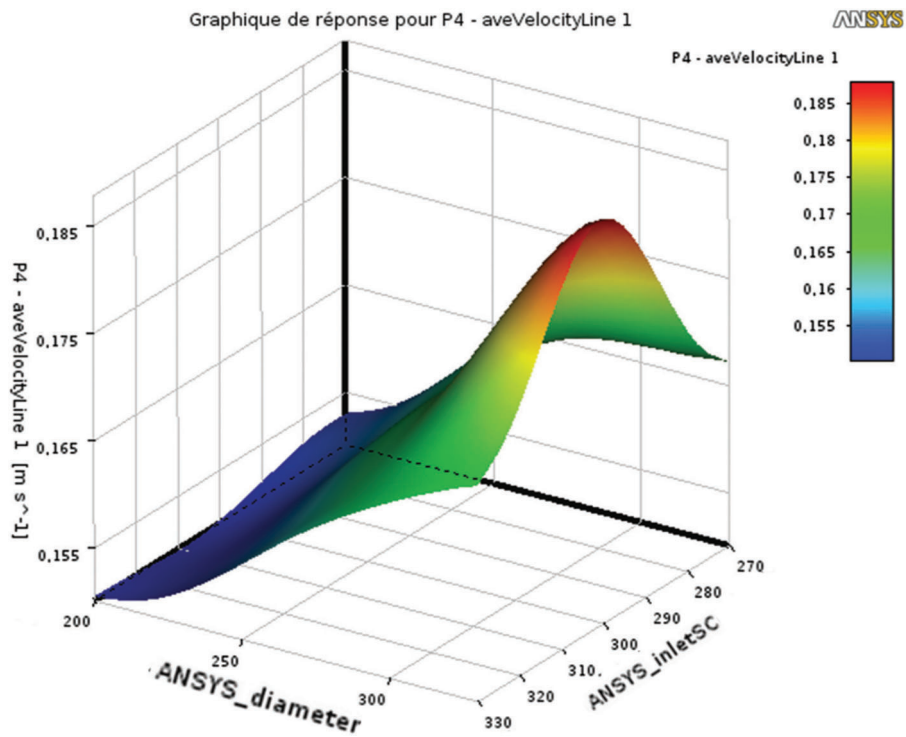
Figure 8: Locale sensibility

Figure 9: Response surfaces of velocity *vs*. solar chimney parameters: Height, tube diameter, absorber length

5 Conclusion

This numerical simulation work applied to a solar chimney with a horizontal absorber is carried out with the CFD Fluent tool on a building model. The results of the simulation of a passive ventilation system with a solar chimney show:

- The velocity distribution in the working area is more significant than 0.2 m/s. This value is sufficient if the average radiant temperature of the walls is not high.
- This new configuration protects the roof of the building from the sun's rays. The shading of the roof is a definite advantage for the comfort of the building.
- The most influential geometric parameter is the outlet diameter of the chimney; it follows the height of the chimney and the length of the absorber.

For optimization, we find that the increase in the outlet diameter and the chimney's height influence the velocity.

We intend to make an experimental validation of our numerical model in the prospects.

Conflicts of Interest: The authors declare that they have no conflicts of interest to report regarding the present study.

References

1. Ahmed, A., Ahmed, A. S., Mona, G. I., Abbas, E. Z. (2019). Solar chimney optimization for enhancing thermal comfort in Egypt: An experimental and numerical study. *Solar Energy, 180,* 524–536.
2. Kasaeian, A., Molana, S., Rahmani, K., Wen, D. (2017). A review on solar chimney systems. *Renewable and Sustainable Energy Reviews, 67(8),* 954–987. DOI 10.1016/j.rser.2016.09.081.
3. Tesfaye, A. (2018). *Design and development of low power output solar chimney power plant.* Ethiopia: Addis Ababa Institute of Technologschool of Gradute.
4. Kinan, A., Sidik, N. A. C. (2016). Experimental studies on small scale of solar updraft power plant. *Journal of Advanced Research Design, 22(1),* 1–12.
5. Balijepalli, R., Chandramohan, V., Kirankumar, K. (2019). Development of a small scale plant for a solar chimney power plant (SCPP): A detailed fabrication procedure, experiments and performance parameters evaluation. *Renewable Energy, 148,* 247–260.
6. Nsaif, O., Ayli, E., Yapıcı, E. Ö. (2020). Numerical investigation on the performance of a small scale solar chimney power plant for different geometrical parameters. *Journal of Cleaner Production,* 122908.
7. Azizi, A., Tahri, T., Segnic, S. M. H. L., Belakroum, R., Loudiyi, K. (2019). Experimental and CFD investigation of small-scale solar chimney for power generation, case study: Southeast of Algeria. *Desalination and Water Treatment, 160,* 1–8. DOI 10.5004/dwt.2019.24167.
8. Nguyen, Y., Wells, J. (2019). A numerical study on induced flowrate and thermal efficiency of a solar chimney with horizontal absorber surface for ventilation of buildings. *Journal of Building Engineering, 28(2),* 101050. DOI 10.1016/j.jobe.2019.101050.
9. Layeni, A. T., Waheed, M. A., Adewumi, B. A., Bolaji, B. O., Nwaokocha, C. N. et al. (2020). Computational modelling and simulation of the feasibility of a novel dual purpose solar chimney for power generation and passive ventilation in buildings. *Scientic African, 8(2),* e00298. DOI 10.1016/j.sciaf.2020.e00298.